Anatomical Substrates for Functional Columns in Macaque Monkey Primary Visual Cortex

Jennifer S. Lund[1], Alessandra Angelucci[1] and Paul C. Bressloff[2]

[1]Moran Eye Center, University of Utah, 50 North Medical Drive, Salt Lake City, UT 84132, USA and [2]Department of Mathematics, University of Utah, 155 S. 1400 E. Salt Lake City, UT 84112, USA

In this review we re-examine the concept of a cortical column in macaque primary visual cortex, and consider to what extent a functionally defined column reflects any sort of anatomical entity that subdivides cortical territory. Functional studies have shown that columns relating to different response properties are mapped in cortex at different spatial scales. We suggest that these properties first emerge in mid-layer 4C through a combination of thalamic afferent inputs and local intracortical circuitry, and are then transferred to other layers in a columnar fashion, via interlaminar relays, where additional processing occurs. However, several properties are not strictly columnar since they do not appear in all cortical layers. In contrast to the functional column, an anatomically based cortical column is defined most clearly in terms of the reciprocal connections it makes, both via intra-areal lateral connections and inter-areal feedback/feedforward pathways. The column boundaries are reinforced by interplay between lateral inhibition spreading beyond the column boundary and disinhibition within the column. The anatomical column acts as a functionally tuned unit and point of information collation from laterally offset regions and feedback pathways. Thalamic inputs provide the high-contrast receptive field sizes of the column's neurons, intra-areal lateral connections provide their low contrast summation field sizes, and feedback pathways provide surround modulation of receptive fields responses.

Introduction

The cortical column was first described as a functional entity for monkey somatosensory cortex by Mountcastle and colleagues (Mountcastle, 1957; Powell and Mountcastle, 1959) and then in primary visual cortex of cat and monkey by Hubel and Wiesel (Hubel and Wiesel, 1962, 1974a,b, 1977). These investigators were struck by the fact that they encountered similar response properties in columns of neurons between pia and white matter, but that properties changed with tangential recording tracks traveling across the cortical sheet. In the visual cortex of the macaque monkey, the diameter of the functional column is hard to define. Some properties, for instance orientation specificity, change gradually in a gradient fashion, such that every sideways shift of the recording point through the cortex, even if not much greater than the diameter of a single cell body, brings a shift in peak orientation tuning of the neurons recorded. At much larger spatial intervals, abrupt changes in orientation occur, interrupting these smooth changes.

An early method used to try and visualize the locus of particular cortical functions was the accumulation of radioactively labeled 2-deoxyglucose (2DG) (Sokoloff *et al.*, 1977). This method showed that regularly sized and regularly spaced columns or slabs of higher metabolic activity could be visualized histologically in the cortex after the animal had been exposed binocularly or monocularly *in vivo* to visual stimulation with a single orientation (see Fig. 1) (Hubel *et al.*, 1978; Humphrey and Hendrickson, 1983). The diameter of these labeled columns or width of slabs, which emerge from a continuously labeled layer 4C after binocular stimulation and stretch from pia to white matter, was found to be ~285 μm with an equal sized zone of lower activity level between them, i.e. center-to-center spacing of labeled columns of 570 μm. This was compared to 385 μm for the width of a single eye ocular dominance band in the same histological tissue (Hubel *et al.*, 1978). The columnar 2DG heavily labeled regions always included the blob zones in layers 2/3 where the koniocellular lateral geniculate nucleus (LGN) thalamic axons terminate. However, it does not appear that it is activity in the K pathway to blobs that is responsible for the 2DG label in the column. At low contrast levels the heavy 2DG label was restricted to layers 4B, 4Cá and layer 6 of the column, and included regions in alignment with the overlying blobs, yet the blob regions in layers 2/3 were inactive (Tootell *et al.*, 1988). Under conditions of high-contrast stimulation with single orientations, cortical tissue was labeled heavily by 2DG in a vertical slab running between the blobs as well as including the blob columns. The 2DG label in the inter-blob regions was presumed, but not proven, to be the locus of neurons responding to the particular stimulus orientation used to drive activity.

With the introduction of optical imaging, surface view functional maps of activity in the most superficial layers (1 and 2) of visual cortex clearly showed progressions through gradually changing orientation preference and abrupt changes in orientation tuning at so-called orientation pinwheels and fractures (Bonhoeffer and Grinvald, 1991; Blasdel, 1992a,b; Obermayer and Blasdel, 1993). The repeat distance of any particular orientation preference measured from these maps was ~640–760 μm *in vivo*. After a correction of +17% to compensate for shrinkage of the histological sections prepared for 2DG, there is a close match between the center-to-center distance of the 2DG columns seen after single orientation stimulation and the mean center-to-center distance of like-orientation regions in optical imaging *in vivo* (700 μm). This implies that the 2DG column covers up to half a full cycle or orientation change, even though it was generated by a single orientation stimulus. We will return to this issue in a later section. Ocular dominance showed well-defined monocular domains when tested by optical imaging, with alternating right and left eye, each of ~450–500 μm width across their narrowest aspect. This alternation reflects the anatomically segregated afferent axon terminal zones of the thalamic relays from each eye forming alternating stripes within layer 4C. However, it becomes harder to define boundaries for ocular dominance columns in superficial and deep layers using physiological recording. Relays from layer 4 to the other layers in cortical depth converge to create gradients of dominance of one eye or the other in binocularly driven neurons across the cortical sheet. Another property, direction selectivity, is known to be sequestered in layers 4B/upper 4Cα and layer 6 within the depth of the column (Hawken *et al.*, 1988) and cannot be readily

© Oxford University Press 2003. All rights reserved.

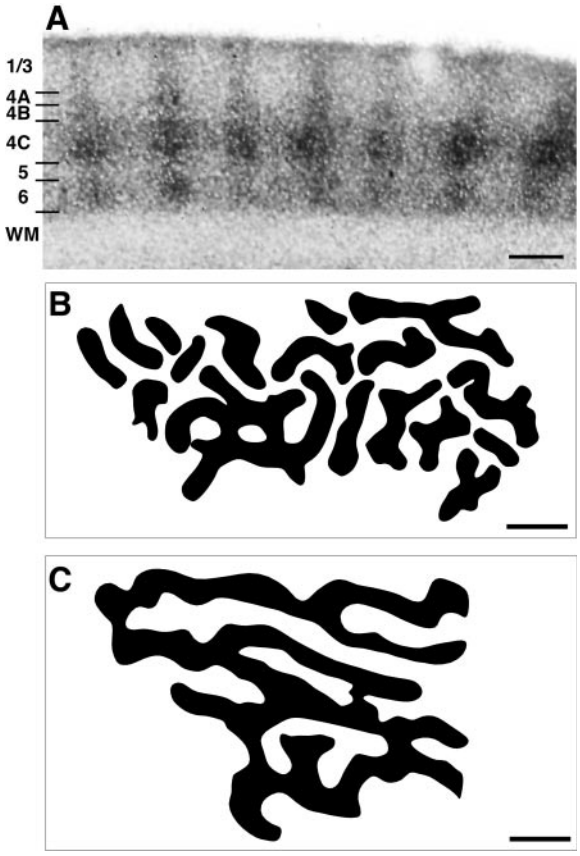

Figure 1. (*A*) 2DG-labeled columns of high activity from an autoradiograph section of macaque monkey visual cortex, area V1. The animal was visually stimulated monocularly *in vivo*, with moving lines of a single orientation. Cortical layers are indicated on the left. Scale bar: 500 μm. Courtesy of A. Hendrickson and A. Humphrey. (*B*) Tangential map of the pattern of heaviest 2DG label in layer 6 of a macaque monkey stimulated binocularly *in vivo* with lines of a single orientation. Traced from patterns in autoradiograph sections illustrated in Hubel *et al.* (Hubel *et al*., 1978). Scale bar: 1mm. (*C*) Tangential map of ocular dominance domains in the same macaque monkey and same region of V1 as in (*B*). The terminal zones for relays of a single eye injected with 3H-proline have been traced from autoradiograph sections illustrated in Hubel *et al*. (Hubel *et al*., 1978). Scale bar as in (*B*).

imaged in the macaque. Thus a number of properties are not the same through the length of the column.

Hubel and Wiesel suggested that the functional columns are grouped into larger entities – or hypercolumns – that encompass representation of all functions (e.g. all orientations and both eyes) within each region of retinotopic space (Hubel and Wiesel, 1974a,b, 1977). In traveling across the cortical retinotopic map there would then be local repeat of retinotopic space for each function, leading to disjunctions of retinotopy. The width of a hypercolumn (suggested to be 1–2 mm) is the distance traveled before entering entirely new visual space, in terms of having no overlap of physiologically mapped receptive fields of neurons in columns at the start point and at the end point. There is, however, no fixed boundary to such hypercolumns, as there is a continuous change in property and mean visual field position across the cortex. Moreover, we now know (Kapadia *et al*., 1999; Sceniak *et al.*, 1999) that the size of receptive fields can increase if low contrast test stimuli are used, rather than the high-contrast stimuli used by Hubel and Wiesel in their studies. Hence, a definition of the hypercolumn size based on receptive field overlap must be qualified, since it depends on how the receptive field is measured.

There are many reasons to reject the concept that a column of cortical tissue is a functional entity, on both physiological and anatomical grounds. The cortical layers have clear differences in organization and function, and seem to represent different processing stages, rather than there being commonality of function or circuitry in cortical depth orthogonal to the layers. Thus, different types of thalamic axons terminate at different depths with clear differences in arbor sizes and functional properties. Cortical laminae, which receive interlaminar relays from different thalamic recipient layers, have clear differences in physiological properties. Efferent projection neurons within different layers connect extrinsically to different regions of visual association cortex or subcortical regions. Lateral connections in each layer of area V1 join together tangentially very different extents of territory across the layer. Moreover, functions that were thought to define a columnar system in primate and cat can exist in mammalian visual cortex without being aggregated into columns. For instance, in the rat visual cortex there are orientation-specific neurons as well tuned as those in primates, but they exist as a salt-and-pepper mix without columnar match in preferred orientation (Girman *et al*., 1999). In the tree shrew, the relays from the two eyes form continuous visuotopic maps in overlying eye-specific layers, rather than being interdigitated within a single layer, as in macaque or cat [see review by Lund *et al*. (Lund *et al*., 1985)]. There is binocular fusion in other layers of tree shrew visual cortex without any laterally offset ocular dominance segregation. This raises the question of what importance to visual information processing in the cortex is functional homogeneity in depth, with regular change tangentially.

In the present review we re-examine the concept of a cortical column in macaque primary visual cortex, and consider to what extent a functionally defined column reflects any sort of anatomical entity that subdivides cortical territory. Is there any meaning for the term cortical 'column' other than the statement that some properties are similar in depth at any particular point across the macaque cortex? Exactly what dimensions do anatomical circuits obey, and what relationship do they have to functions recorded physiologically from single neurons at all depths, or to optically imaged activity patterns in the most superficial stratum of the cortex? While considering these questions, we should remember that comparison of dimensions obtained using different experimental methods has some degree of inaccuracy.

Thalamic Axon Fields: Do They Create a Scale for Functional and Anatomical Match in Column Size?

To begin answering the above questions, it is useful to consider the very first steps of information processing in the visual cortex, the thalamocortical links, and how they may influence the dimensions of concurrently active pools of neurons in the cortex. The largest of the thalamocortical axons are those from the magnocellular, M, division of the LGN. The largest measured terminal fields of single M axons have a spread of 1.2 mm in upper layer 4Cá, and single axon terminal fields can bridge up to three ocular dominance stripes for the same eye (Blasdel and Lund, 1983). The post-synaptic spiny stellate neurons receiving M input have a dendritic field diameter of ~200–250 μm. One such cell could therefore get direct thalamic inputs from a field of overlapped M axon fields with total diameter matching the equivalent of about two side-by-side abutting, but non-overlapping, M axons, i.e. ~2.4 mm (assuming that the axons must cover and provide synapses to at least half the dendritic arbor to be an effective drive). Since a perfect retinotopic map

can be recorded in the positions of circularly symmetric receptive fields of individual neurons recorded sequentially in tangential tracks through layer 4Cα (Blasdel and Fitzpatrick, 1984), it seems reasonable to assume that the spread of single M axons across cortex represents the retinotopic size of the thalamic neuron's effective receptive field. Interestingly, the largest minimum response fields and peak spatial summation fields of V1 neurons, measured at high contrast, match the retinotopic size of the M axon field offered to the single layer 4C cell (Angelucci *et al.*, 2000, 2002a,b; Levitt and Lund, 2002). One would have to travel ~1.2 mm with a recording electrode tangentially across cortex to encounter another cell whose M inputs have no common response field territory with M inputs to cells at the start point.

Neurons through the depth of layer 4C show a gradient of decreasing minimum response field (mrf) size from the top to the bottom of the layer (Blasdel and Fitzpatrick, 1984). The size of the mrf recorded using small high-contrast single bar stimuli seems to depend on the overall weight of M versus P input that the postsynaptic 4C neurons receive. This is presumably due to the fact that their dendrites spread to different degrees into the terminal zones of both M and P axons, depending where they lie

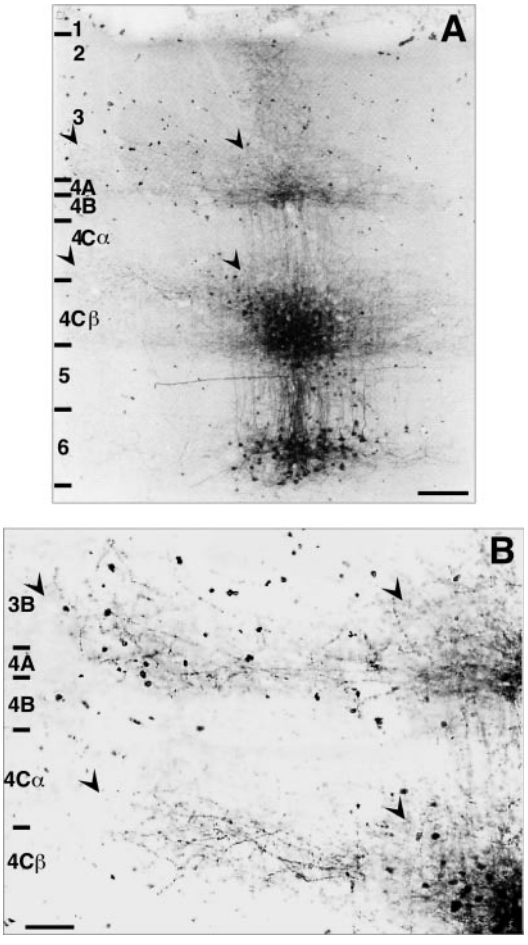

Figure 2. (*A*) Biocytin injection in layer 4Cα under an inter-blob region of layers 2/3. Labeled fibers rise vertically to terminate heavily in layers 2A and 3. Arrowheads indicate the origins and termination zones of lateral projections in mid layer 4C and in deep layer 3. These same zones are shown at higher power in (*B*) (arrowheads). These lateral projections make terminal clusters offset laterally by 300–350 μm from the injection axis. Scale bars: 100 μm (*A*), 50 μm (*B*). Modified from Yoshioka *et al.* (Yoshioka *et al.*, 1994).

in depth of the 4C layer (Bauer *et al.*, 1999). Contrast sensitivity decreases from top to bottom of the layer in proportion to decreasing receptive field size. The smallest mrfs are seen in those neurons receiving purely P inputs in lower 4Cβ. The postsynaptic spiny stellate neuron dendritic arbors are ~200 μm in diameter, matching the diameter of individual P thalamic axon arbors in 4Cβ (individual P axons have about one-sixth the spread of single large M arbors, that is, ~200 μm). The total diameter of the field of terminations of P axons overlapping at least half the dendritic field of single spiny stellate neurons is therefore ~400 μm.

The M and P axons innervating layer 4C thus generate an orderly retinotopic map that is maintained vertically throughout the layers of V1. This could lead to the notion of a 'retinotopic column' based on the minimum distance between cortical points with non-overlapping receptive fields. However, one must be careful with this definition of a column, since, as we mentioned earlier, the physiologically measured size of a receptive field depends on the method used to measure it. V1 neuron receptive fields, measured by expanding high-contrast grating stimuli, are a good match to the visuotopic extent of M thalamic inputs offered to their home cortical 'column'. However, if low contrast stimuli are used, it has been shown that single cortical neurons can sum inputs over an area 2–3 times larger than when high-contrast stimuli are used (Sceniak *et al.*, 1999). The anatomical routes by which the neuron can gain access to this large summation field were addressed by us in recent work (Angelucci *et al.*, 2002a,b). We showed that long-range lateral connections, innervating any single point across cortex, arise from a cortical field of cells in either layers 2/3 or layers 4B/4Cα measuring on average 6 mm in longest diameter. These lateral connections provide any small point in these layers with access to information from neurons with an aggregate receptive field that matches the low contrast summation fields of single neurons. The lateral connection field is 2–3 times larger than the field offered by direct thalamic input to any local 'column' of 250–300 μm diameter.

Local Cortical Circuits: Do They Form a Substrate for 'Functional' Columns?

Orientation Selectivity

The mrfs of layer 4C neurons with circularly symmetric receptive fields constitute a single retinotopic map laid out tangentially across the layer. Receptive fields are also perfectly aligned across the depth of layer 4C despite differences in mrf size at different depths in the layer (Blasdel and Fitzpatrick, 1984). In the same 4C layer, neurons that have orientation specificity, direction specificity and binocularly driven responses first appear in cortex (Hawken and Parker, 1984; Hawken *et al.*, 1988). So the substrates for generating all of these properties almost certainly lie within the 4C layer. The generation of orientation specificity is generally thought to involve the convergence to single neurons of retinotopic information distributed along their axis of preferred orientation. In cat, this convergence is believed to be from LGN axons to single layer 4 neurons (Hubel and Wiesel, 1977; Reid and Alonso, 1995). However, in macaque monkey it is more likely to occur between neurons lying at different positions across the retinotopic map in layer 4C, as suggested by the latency with which layer 4C neurons develop an orientation-tuned response – ~10 ms after the beginning of the response (Ringach *et al.*, 1997).

Within the middle depth of layer 4C, where single neurons receive both M and P inputs, anisotropic lateral projections are

made by the excitatory spiny stellate neurons (Fig. 2) (Anderson *et al.*, 1993; Yoshioka *et al.*, 1994). These projections lie within the cortical retinotopy of the receptive field of single mid-4C neurons, making terminal clusters ~200–250 μm in diameter at points offset by 300–600 μm from the neurons of origin. The terminal patterns are spatially oriented, since they occur as projections to just one point to one side of the parent neuron, to two points on opposite sides, or to several clusters on one side and one cluster on the other (Anderson *et al.*, 1993). These small-scale lateral projections can be accompanied by laterally offset projections to layer 3B (Fig. 2*B*) from neurons at the same locus in layer 4C. The terminal fields in layer 3B are in vertical alignment with the offset patches of terminals in mid layer 4C in the case shown in Figure 3. It follows that these anisotropic intracortical excitatory lateral connections could start a process of combining circularly symmetric fields to build vertically aligned clusters of orientation-specific neurons in layers 4C and 3B (Lund *et al.*, 1995). The feasibility of such a mechanism has been investigated in a simplified computational model of layer 4C of macaque striate cortex (Adorjan *et al.*, 1999). However, one still needs to establish that a full cycle of orientation preferences can be generated within the spatial extent (600 μm) of the mid-4C lateral connections. The axons of mid-layer 4C excitatory neurons also project locally upward to terminate within upper layer 4Cα, where they could relay their orientation-specificity domains. At this same upper 4Cα level, very extensive (3–4 mm long) lateral projections converge to any small tracer labeled point (Fitzpatrick *et al.*, 1985; Yoshioka *et al.*, 1994; Angelucci *et al.*, 2002a,b). These lateral projections converge from both sets of ocular dominance domains, and are therefore likely to provide the neurons in this layer with their binocular inputs.

We conclude that the orientation map as observed in optical imaging is first generated within layer 4C, and then carried forward to other layers through vertical integration. This leads to the notion of a functional 'orientation' hypercolumn (one full cycle of orientation preference) whose dimension (500–600 μm) is determined by the period of laterally connections between mid-4C neurons. An interesting question is then why the dimension of a 2DG column corresponds to approximately half a cycle variation in orientation selectivity.

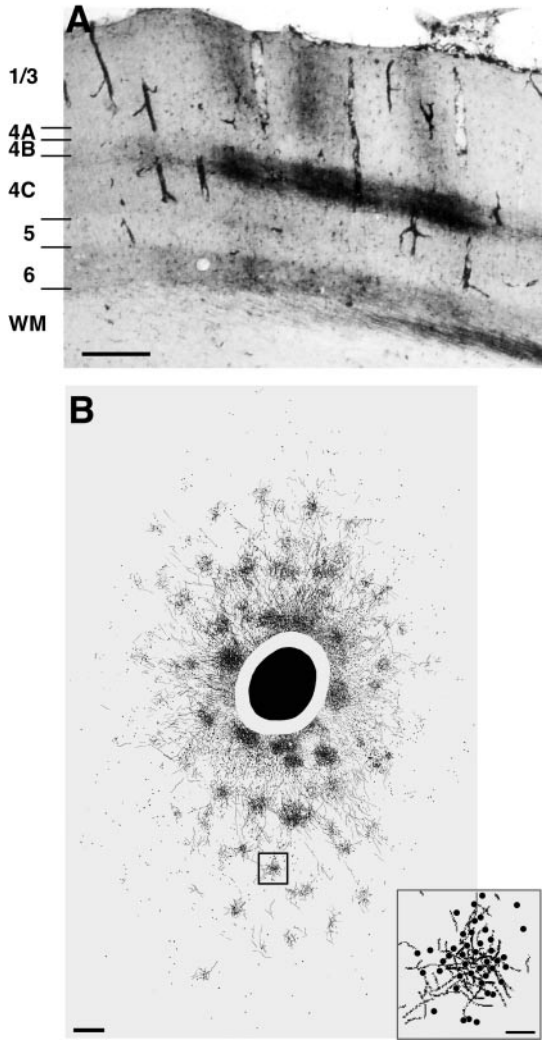

Figure 3. (*A*) Pia to white matter section of squirrel monkey area V1, showing label to the side of a large injection of HRP (not shown) through layers 1–6. Columns of heavy terminal label are seen in layers 1–3; heavy label in layers 4B/upper 4Cα shows higher density under each column of label in layers 2/3; similar increased terminal densities occur in layers 5 and 6 in alignment with the regions of densest label in overlying layers. Scale bar: 100 μm. Modified from Rockland and Lund (Rockland and Lund, 1983). (*B*) Surface view of a 2D composite reconstruction of labeled lateral connections in layers 2/3 of macaque monkey area V1, showing a clustered pattern of anterogradely labeled terminals and retrogradely labeled neurons (inset) surrounding an injection of the tracer CTB (black oval). The patches of terminals and cells are the cross-sections of columns of label of the kind seen in (*A*). Small square: labeled patch shown at higher power in inset. Note that both retrogradely labeled cells and orthogradely labeled terminal axon processes are present in each patch, indicating reciprocity of connections with the injection site. Scale bar: 500 μm. Inset: higher power drawing of patch in small square. Scale bar: 100 μm.

Orientation Tuning and the Role of Inhibitory Neurons

One possible interpretation of the dimension of a 2DG column is that it reflects the width of orientation tuning curves generated by a single oriented stimulus. It is still a matter of debate whether the degree of tuning is determined by the same mechanism that generates the orientation preference, or whether additional sharpening and amplification is produced by local intracortical inhibition. Measurements in cat suggest that the degree of alignment of receptive fields of LGN neurons is sufficient to account for the degree of orientation tuning of simple cells functionally connected to them (Reid and Alonso, 1995). In addition, Ferster *et al*. (Ferster *et al.*, 1997) have shown that cooling a patch of cortex, and therefore presumably abolishing neuronal intracortical activity, does not significantly affect the degree of orientation tuning exhibited by EPSPs generated by LGN input (however, only the tuning of the amplitude of temporal modulations in the voltage was measured, which does not reflect the tuning of the steady-state or mean response). On the other hand, there is also growing experimental evidence suggesting that blockade of extracellular inhibition with bicuculline leads to considerably less sharp tuning (Sillito *et al.*, 1980; Nelson, 1991). It is important to emphasize that this form of inhibitory blockade affects a local population of neurons and can thus disrupt the intracortical processes that contribute to orientation tuning. In contrast, intracellular blockade of a single neuron has a negligible effect on its tuning properties (Nelson *et al.*, 1994), presumably because this more localized blockade does not disrupt the tuning of excitatory neurons that innervate the given cell. Further evidence for the important role of intracortical inhibition is that orientation tuning appears to take up to 50–60 ms to reach its peak, and the dynamics of tuning has a rather complex time course (Ringach *et al.*, 1997).

The possible role of local recurrent cortical interactions in amplifying and sharpening orientation tuning has been analyzed using the so-called *ring model* of a cortical hypercolumn

(Ben-Yishai *et al.*, 1995; Somers *et al.*, 1995), Here the width of a tuning curve in response to a weakly biased input from the LGN is determined by the spatial extent of local intra-cortical inhibition. The computational model of Adorjan *et al.* (Adorjan *et al.*, 1999) is a generalization of the ring model to layer 4C of the macaque, in which intra-cortical connections play a dual role, providing both the initial orientation bias, as described above, and its subsequent amplification. One of the major assumptions of the ring model is that within a hypercolumn, local inhibitory neurons have a larger axonal arborization than local excitatory neurons (as distinct from long-range excitatory neurons, see below). This implies that, at least in the linear zones of the orientation map, inhibition links neurons over a wider range of orientation preferences than excitation. Interestingly, this has received some recent experimental support in the ferret (Roerig and Chen, 2002). Note that an alternative model of orientation tuning in layer 4C of macaque has been developed by McLaughlin *et al.* (McLaughlin *et al.*, 2000), in which sharp orientation tuning is generated under the assumption that local inhibitory interneurons have a smaller axonal arborization than excitatory neurons.

Here we review possible anatomical substrates for local inhibition within the macaque. Our anatomical studies of interneuron morphology have shown each layer to have its unique set of interneurons, though cells of the same morphology can occur in several layers (Lund, 1987; Lund *et al.*, 1988; Lund and Yoshioka, 1991; Lund and Wu, 1997). Interneurons are generally GABAergic and therefore inhibitory or modulatory. Different classes of interneuron specifically synapse onto different regions of the excitatory pyramidal neuron or spiny stellate cell (Somogyi *et al.*, 1998), and can also inhibit other interneurons. The interneurons usually provide a local axon field in the layer of the cell's own dendritic field. Moreover, many project vertically in cortical depth, making specific interlaminar links. Most have dendritic field and axon arbor extents of 300 μm or less in diameter. A few either have extremely narrow (down to 70 μm) vertically arrayed axon fields or have axons that project tangentially across cortex, outside the local environment of their dendritic arbor (but still not nearly as far as lateral projections of the excitatory neurons).

We have suggested previously (Lund *et al.*, 1993) that a particular set of basket neurons in layers 4B–3B, whose dendritic fields fit within the 2DG column diameter, but whose axons spread three times a column diameter, could exert an appropriately scaled inhibitory field to silence pyramidal neurons in adjacent non-active columns. It is known that these basket neurons contact pyramidal neuron somata and proximal dendritic segments, and that they contact each other to provide mutual inhibition (Somogyi *et al.*, 1983), thus providing an inhibitory substrate for sharpening the column boundaries and the tuned response (as assumed in the ring model, see above). Adorjan *et al.* (Adorjan *et al.*, 1999) take inhibition to be more broadly tuned than excitation, whereas McLaughlin *et al.* (McLaughlin *et al.*, 2000) assume the opposite is true. In the cat, wide-arbor basket neurons of upper layer 4 and deep layer 3 have been studied extensively (Buzas *et al.*, 2001), since their processes label with even extracellular deposits of tracer, unlike the finer processes of the monkey neuron GABA cells. The distal processes of the axon arbors of the cat basket neurons cover territory of all orientation specificities, but favor territory of the opposite orientation specificity from that occupied by their dendritic territory. These cells seem morphologically most similar to the layers 4B–3B wide-arbor basket neurons of type 4B:3, or 3B:3 in macaque (Lund and Yoshioka, 1991).

Wide-arbor basket neurons are found at all depths in V1 but layer 4Cβ. This raises the interesting question as to whether they could be the source of inhibition assumed to play a role in models of orientation tuning in layer 4C. In mid-4C there are interneurons of basket neuron type with anisotropically distributed, laterally running longer axon collaterals [neuron variety α4 (Lund, 1987)]. The interplay between the wide-arbor basket neurons, with axons spreading beyond the column, and modulatory interneurons, having both axons and dendrites confined to the 2DG column boundaries, should help define the borders of active and inactive columns. Activity driven by the thalamic afferents not only drives the column's excitatory neurons but also the inhibitory neurons. The inhibitory neuron intracolumnar circuits include projections between layers that follow the column's excitatory circuits. Forward-running inhibition within the column could disinhibit the targets of the excitatory intracolumn relays by suppressing the activity of inhibitory neurons controlling them. These intracolumnar disinhibitory circuits would help to promote activity in specific pathways within the active column, while longer lateral inhibition spreading into neighboring columns could suppress the surrounding activity, thereby increasing the difference in activity levels between neighboring columns.

Direction Selectivity

Another response property that first appears in upper layer 4C is direction selectivity (Hawken *et al.*, 1988). This property is linked to orientation specificity, since the axis of direction specificity is orthogonal to the cells' axis of orientation preference. How is direction specificity generated in this layer? Upper layer 4Cα receives input from the largest population of M axons and projects to layer 4B. Both layers share a common population of basket interneurons of types α:6 and 4B:6 (Lund, 1987; Lund and Yoshioka, 1991) whose dendritic extent matches that of the excitatory neurons (~200–250 μm), but whose very long, stout axon trunks spread tangentially up to 750 μm from the soma. It is possible that these lateral inhibitory projections underlie the generation of direction selectivity, a property shared by both cortical layers (Lund *et al.*, 1995). Laterally within cortex, the distance between the inhibitory cell dendritic field center and its furthest axon terminals is compatible with the largest retinotopic separation of sequentially illuminated pairs of static dot stimuli that can generate direction selective responses from single V1 neurons [~0.2° at 4° eccentricity = cortical distance of 230–580 μm, or 0.8° at 20° eccentricity = cortical distance of 290–456 μm (Newsome *et al.*, 1986)]. The first dot stimulus could generate fast-conducting, laterally spreading inhibitory input to neurons offset across the cortical sheet, which could veto the subsequent response to the second dot image arriving at the veto point. The conduction velocity of the inhibition, together with its degree of spatial asymmetry, would determine the effective direction tuning curve. It is clear that direction selectivity is accomplished within the same framework as the generation of orientation specificity, within the retinotopy of the single 4C neuron mrf, but that it is added to neuron response properties within upper layer 4Cα. Orientation specificity is present in layer 3B without direction specificity, so while the projections from mid-4C to layer 3B may carry orientation specificity, they presumably arise from neurons lacking direction specificity.

Spatial Frequency Selectivity

There is considerable physiological and psychophysical evidence to suggest that cortical cells act like band-pass filters for both orientation and spatial frequency, so that cells carry out a

localized two-dimensional spatial frequency filtering of a stimulus rather than simply performing local edge detection [for a review, see deValois and de Valois (deValois and de Valois, 1988)]. The distribution of spatial frequency preferences across cortex is less clear than that of orientation.

Early findings by Hubel and Wiesel (Hubel and Wiesel, 1962) revealed numerous cells in cat with poor to no tuning for orientation, and similar cells were later located in cytochrome oxidase (CO) blob regions of monkey V1 (Livingston and Hubel, 1984a). These are now thought to be regions of low spatial frequency preference (Hubener *et al.*, 1997). More recent optical imaging studies in cat (Hubener *et al.*, 1997; Issa *et al.*, 2000) suggest that both orientation and spatial frequency are distributed almost continuously across cortex, spatial frequencies at the extremes of the continuum tend to be located close to orientation pinwheels (sites of rapid change of orientation preference), and around the pinwheels iso-orientation and iso-frequency contours are approximately orthogonal. These particular features have been incorporated into a generalization of the ring model, in which local recurrent interactions generate both sharp orientation and spatial frequency tuning within a hypercolumn (Bressloff and Cowan, 2002b).

The precise relationship between spatial frequency preference maps, CO blobs and orientation pinwheels remains a controversial issue. The situation is even less clear in macaque, where M and P axons target distinct layers suggesting, perhaps, that high and low spatial frequency preferences may be separated into layers rather than spread tangentially across cortex. On the other hand, the finding that lateral connections in certain inter-blob regions can be less extensive than blob regions (see later) (Yabuta and Callaway, 1998) is consistent with the notion that the regions lacking longer connections might be associated with regions of high spatial frequency and those with longer lateral connections may be regions with lower spatial frequencies.

Excitatory Lateral Connections: Linking Up Functional and 'Anatomical' Columns

Superficial Layers 2/3

Many of the excitatory pyramidal neurons in the superficial layers 2/3 of area V1 send long-range, tangentially spreading lateral connections within the layer, forming periodic patches of terminals (Fig. 3) contacting both excitatory and inhibitory cells (McGuire *et al.*, 1991). These connections are reciprocal, since injections of bi-directional tracers in these layers additionally retrogradely label somata within the terminal patches (Fig. 3*B*, inset). The 2DG-labeled orientation column or slab width matches the average spread of the dendritic field of single pyramidal neurons within the column, as well as the size of patches of terminals provided by lateral connections in the superficial layers 2/3 (Rockland and Lund, 1983). Interestingly, across a variety of cortical areas in different species, columnar patchy lateral connectivity is common; however, while terminal column size varies between areas and species, there is a constant relationship between the average single excitatory neuron dendritic extent and column size for each area (Lund *et al.*, 1993). The patchiness of lateral connections is also visible in deeper layers, and columnar alignment of labeled patches occurs in depth (Fig. 3*A*), resembling the 2DG-labeled functional column (Rockland and Lund, 1983). These lateral connection terminal fields are, perhaps, the only clearly identifiable example of 'anatomical' columns.

The lateral connections form a continuum in cortex, in that each lateral shift in injection locus will shift the location of the offset labeled points connected to it. Thus, while the columns of terminals have definite boundaries, they are defined by what connects to them and what they connect to tangentially across the cortex. They do not have unique occupancy of a 250–300 μm diameter column of cortical tissue – many other columns share portions of the same territory. Anatomy combined with optical imaging shows that the columns that are interconnected are largely (60–70% match) regions of common property [common ocular dominance, orientation preference, or blob to blob k input zones (Malach *et al.*, 1993; Yoshioka *et al.*, 1992, 1996; Yabuta and Callaway, 1998)].

One surprising observation is that even large injections of tracer, with uptake zones covering several repeats of any function, result in offset labeled columns with the same size and spacing as those produced by small (300 μm in diameter) injection sites. Why is there almost no 'filling in' of the gaps between columns of label when several neighboring repeats of all functions are injected with biocytin or cholera toxin B (CTB) tracers? One suggestion we can make is that uptake and transport of the label depends on activity level. It may be that only one functional set of columns can be active at any one time *in vivo*, and that the activity in that set drives inhibition, thus lowering activity in alternate columns. If so, even with large pressure injections of anatomical tracer, cortical activity during the phase of tracer uptake might be captured by the active set of columns and this produces the pattern seen in histology. In fact, there is evidence from optical imaging of visual cortex, that when no stimuli are offered, the cortex shows activity patterns that resemble those seen under conditions using single orientation stimulation (Tsodyks *et al.*, 1999). This supports the possibility that only single sets of columns can be active at any one time, even when the cortex is not driven by external visual stimulation. It has recently been suggested that these spontaneously generated activity patterns could form the basis of geometric visual hallucinations (Bressloff *et al.*, 2001). Interestingly, the fundamental length-scale of common hallucinatory images, when mapped into cortex, matches the dimension of the hypercolumn.

When very large injections of the older, more diffusible tracer horseradish peroxidase (HRP) were made in our earlier studies (Rockland and Lund, 1983), more filling in of the pattern of lateral connections was seen (Fig. 4). This filling in was most

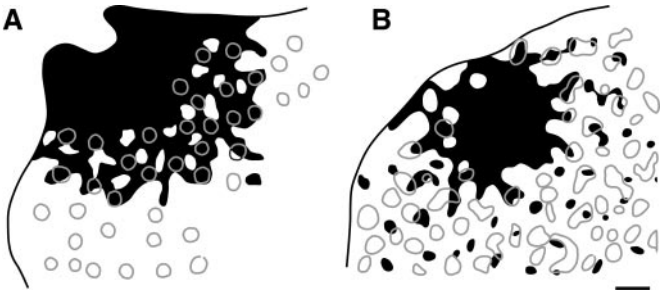

Figure 4. Tangential maps of labeled terminal zones in layers 2/3 (black regions) surrounding large injections of HRP in squirrel monkey (*A*) and macaque monkey (*B*) primary visual cortices. The position of CO-rich blobs (gray contours) are indicated. It is noticeable that in moving away from the center of the injection site (solid black), a pattern of lightly labeled lacunae (white areas) first appears, followed by arm-like protrusions of label, and then by a pattern of isolated terminal patches (mapped in the macaque). The CO blobs tend to lie in the solidly labeled walls around the lacunae. Modified from Rockland and Lund (Rockland and Lund, 1983). Scale bar: 500 μm.

marked in the squirrel monkey V1, but also occurred in macaque. In tangential view of layers 2/3, the label created heavily labeled walls of terminal processes around sparsely labeled lacunae. The diameter of the lacunae was about the same as the width of the walls (200–300 μm), and the CO blobs lay within the heavily labeled walls. The overall picture in tangential view looked somewhat like the 2DG patterns produced from binocular stimulation with a single orientation (Fig. 1*B*) (Hubel *et al.*, 1978). A correlate may be the finding of Yabuta and Callaway (Yabuta and Callaway, 1998) that there exists a population of pyramidal neurons, positioned between 130 and 200 μm from blob centers, that does not make long laterally spreading patchy connections, but confines their axon arbors largely to within 600 μm of their cell body in the inter-blob regions. Perhaps these neurons lie within the lacunae of the HRP label patterns, within columns that occupy part of the inter-blob regions and that neither make nor receive long lateral connections. It has been reported (Yousef *et al.*, 2001) that the pinwheel zones in cats connect more locally and diffusely than the linear zones of orientation change. We have observed a similar connectivity pattern in ferrets (A. Angelucci, S. Sharma and M. Sur, unpublished observations). So perhaps the lacunae in the monkey connectivity patterns are pinwheel zones corresponding with the high spatial frequency regions as discussed earlier.

It is known that excitatory inputs from columns of lateral connections, and from feedback pathways from extra-striate cortex (that are specifically directed to columns of the same 250–300 μm diameter, see below), can suppress activity of neurons in the column. We have suggested (Angelucci *et al.*, 2002a) that this suppression results from an excess level of excitation reaching the column via a combination of feed-forward thalamic, lateral excitatory and feedback pathways. The sum of these inputs could raise the activity of local inter-neurons sufficiently to allow their inhibitory inputs to the local excitatory cells to effectively lower their firing rate (Lund *et al.*, 1995). The facilitatory impact of lateral excitatory pathways to the column neurons becomes more evident as input from thalamic afferents to the column is lowered, by either reducing the stimulus contrast, or by eliminating direct thalamic input to the column altogether, as with retinal lesions or artificial scotomata. Expansion of the stimulus then adds excitation to the column via lateral connections. After creation of a scotoma that silences thalamic input to a region of visual cortex, there is a rapid period of increase in efficacy of the synaptic inputs from these alternative sources of excitatory inputs to the column (Gilbert and Wiesel, 1992; Das and Gilbert, 1995; Calford *et al.*, 1999). So these lateral connections remain plastic in terms of their impact on the column, and appear to be able to rapidly adjust that impact in response to changes in the column's other inputs.

Some of the above ideas have been implemented in computational models examining how the interaction between local and long-range circuitry contributes to the response properties of cortical cells (Somers *et al.*, 1998; Dragoi and Sur, 2000; Stetter *et al.*, 2000; Bressloff and Cowan, 2002a). In these models the local circuitry generates sharp orientation tuning along the lines of the ring model (see above), which is then modulated by lateral interactions linking different hypercolumns. Following the original proposal of Lund *et al.*, local high-gain inhibitory cells are shown to provide one mechanism for the contrast-dependence of the inhibitory surround (Lund *et al.*, 1995). Although these models assume that surround suppression is mediated by lateral connections, it should be possible to extend the models to incorporate feedback from extra-striate areas (see below) (Angelucci *et al.*, 2002a).

Layers 4B/upper 4Cα

In layer 4B, and in upper 4Cα postsynaptic to the largest M thalamic inputs, our preliminary studies suggest that the tangential connectional architecture differs in pattern from that seen in the superficial layers 2/3 (Asi *et al.*, 1996) (A. Angelucci, J.B. Levitt, P. Adorjan, Y. Zheng, L. Sincich, N. McLoughlin, G.G. Blasdel and J.S. Lund, unpublished data). At this deeper level the terminals and cells contributing to tangential connections in layers 4B and upper 4Cα are arrayed in bands surrounding any small tracer injection (Fig. 5). The bands of terminals are the same width as the diameter of the columns of terminals in layers 2/3, and gaps of equal width occur between the bands. The columns of terminals of lateral projections in layers 2/3 are aligned vertically along the bands in layers 4B/upper 4Cα, when both are labeled by columnar tracer injections. With the admittedly uncertain assumption that the surface optical map is applicable to these deeper layers, it appears, from aligning sections of anatomical label with optical maps, that the bands include territory favoring orientations matching those of the overlying layer 2/3 columns and injection site, but with broader orientation tuning. The bands also include equal territories for the two eyes, regardless of the location of the injection site, whereas the layer 2/3 connections favor the same ocular dominance territory as that of the injection site. These differences in the pattern of lateral connections between layers 2/3 and 4B/upper 4Cα might reflect corresponding differences in functional tuning or in functional maps, for example, direction selectivity. The combination of M inputs (giving lower acuity, but higher contrast and temporal sensitivity than P inputs), wide spreading excitatory lateral connections (creating binocular neurons in the same layer receiving direct monocular thalamic inputs) and unique widely spreading inhibitory substrates may all underlie the more broadly tuned functional sampling from offset columns in layers 4B/upper 4Cα compared to the superficial layers 2/3.

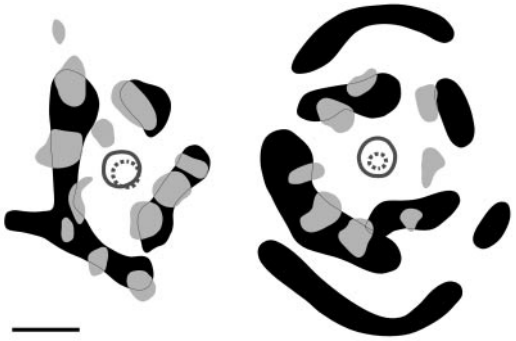

Figure 5. Two examples of composite reconstructions of terminal label surrounding single columnar injections of biocytin involving layers 2/3 and 4B/upper 4Cα, obtained by overlaying serial tangential sections of macaque monkey V1. Black bars: terminal zones in layers 4B/upper 4Cα. Gray patches: terminal label in layers 2/3. Hatched circles: tracer uptake zone in layers 2/3. Unbroken circles: tracer uptake zone in layer 4B/upper 4Cα. Note the overlap of the layer 2/3 patches with the layer 4B/upper 4Cα terminal bars. These two cases showed no regular alignment with the CO blobs [not shown (A. Angelucci, J.B. Levitt, P. Adorjan, Y. Zheng, L. Sincich, N. McLoughlin, G.G. Blasdel and J.S. Lund, unpublished data)]. Scale bar: 500 μm.

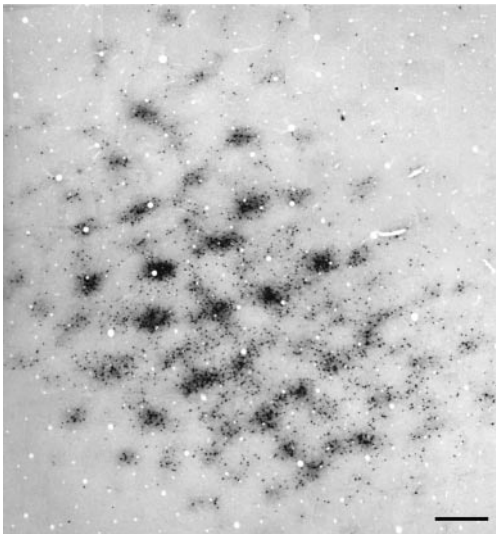

Figure 6. Bright-field photomontage of a tangential section through layer 4B of macaque area V1, showing CTB-labeled cell bodies (cells of origin of feedforward projections to extra-striate cortex) superimposed on terminal fields (terminal zones of feedback projections from extra-striate cortex), resulting from an injection site in dorsal area V3. Note the patchy pattern of inter-areal connections. Scale bar: 500 μm.

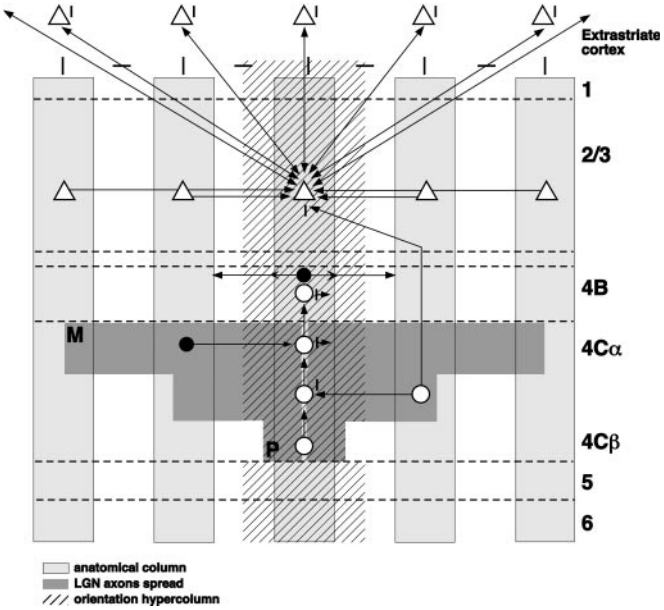

Figure 7. Schematic diagram of the anatomical and functional cortical columns in macaque V1. Light gray zones: anatomical columns (terminal zones of lateral connections); these match in size with heavily labeled 2DG functional columns after *in vivo* stimulation with vertical line orientations (indicated by vertical line symbol). Hatched region: scale of one complete orientation cycle (an orientation hypercolumn; here, center-to-center of horizontal orientation-specific regions – marked by horizontal bar symbol). Dark gray zone: gradually widening zone from bottom to top of layer 4C of thalamic input to the center column's neurons. These inputs provide the substrates for the size of 4C neurons high-contrast receptive fields. P: purely parvocellular LGN inputs. M: widest zone of purely magnocellular LGN inputs. In the middle depth of layer 4C, where neurons share both M and P inputs, a spiny stellate neuron (open circle) makes a single lateral step excitatory connection that creates vertical orientation preference in the spiny stellate neuron of the center column (open circle). The latter neuron projects vertically to upper layer 4Cα, where lateral inhibition (filled black circle) adds direction specificity to orientation (marked by vertical bar with attached arrow). Both response properties are then relayed to layer 4B neurons. Within 4B, orientation tuning and the column structure become more pronounced under the influence of long-range inhibition exerted by wide-arbor basket neurons (filled black circle in 4B). The same offset spiny stellate neuron in mid-4C that gives the center 4C column its orientation specificity also provides input to layer 3 of the same column; thus, the vertical orientation preference (but not direction preference) is given to the column at this level. Extensive intracortical lateral excitatory inputs to the center column arise from pyramidal cells (open triangles in layers 2/3) within functionally matching columns. These are only shown in layers 2/3, although they are present in layers 4B/4Cα and layers 5 and 6. Lateral connections converge to the center column from a cortical territory of ~3 mm radius. Feedback neurons (open triangles in extra-striate cortex) of matching orientation (vertical bar) specificity relay information to the center column from more extensive regions of visual space than intra-areal lateral connections. These connections show columnar and lamina specificity, and could provide a substrate for long-range surround modulation of center neuron responses.

Relationships Between the Anatomical Column and Feedforward and Feedback Connections with Extra-striate Cortex

We know from our own work and that of others (Lund *et al.*, 1975; Livingstone and Hubel, 1984b; Shipp and Zeki, 1989; Angelucci *et al.*, 2002a,b) that efferent neurons in area V1 projecting to different external destinations are sequestered in different layers, and that within single layers efferent neurons projecting to particular compartments in extra-striate areas are organized in small clusters (Fig. 6). Moreover, feedback connections from extra-striate cortex target the clusters of neurons that provide feedforward projections to the same extra-striate site. These clusters of feedforward cells and feedback terminals have the same diameter in the tangential plane as the intrinsic lateral connectivity columns in layers 2/3, the CO blobs, and the width of intrinsic connectivity stripes in 4B. The inter-areal connections, therefore, seem to be a component of the same V1 anatomical column system as the intrinsic connections. There is considerable convergence of visual information to single cortical columns from this extra-striate feedback. We have shown that the size of physiologically recorded modulatory surround fields for single V1 neurons (Levitt and Lund, 2002) are too large to be provided purely by monosynaptic intra-areal fields. However the sizes of surround fields are compatible with the visuotopic extent of feedback connections to single V1 columns (Lund *et al.*, 1999; Angelucci *et al.*, 2002a,b). In addition, it is known that these inter-areal connections are very fast conducting compared to intra-areal connections (Girard *et al.*, 2001), and that they do indeed play a role in modulating the responses of V1 neurons to stimuli within their receptive field (Hupé *et al.*, 1998). There may, however, be a difference between the efferent feedforward neuron column system and the intra-areal lateral connection columns. We made the point above that the intra-areal lateral connection columns appear to be a continuum across cortical territory. However, at least one of the sets of efferent cell clusters are in fixed-place columns, those that are contained in the CO blobs. These blob zones contain populations of neurons that project to the thin, CO-rich stripe compartments within V2 (Livingstone and Hubel, 1984a; Sincich and Horton, 2002). To what degree the other efferent neuron sets, projecting to specific compartments in extra-striate areas, are confined to particular, fixed-place V1 columns, or obey the continuously distributed pattern such as the orientation-specific column system (Schmuel *et al.*, 1998) is, as yet, unclear.

Conclusions

We have reviewed the historical concept of a functional column and tried to identify its anatomical correlate in the primary visual cortex of the macaque monkey. We summarize our concept of the relationship between the anatomical and functional column in Figure 7. Physiological recording, 2DG and optical imaging studies have shown that functional columns relating to different properties are mapped in cortex at different spatial scales.

Furthermore, several of these properties are not strictly columnar in the sense that they are not present within all cortical layers. Anatomically speaking, the circuitry underlying a functional column is often not 'visibly' columnar, but rather appears to reflect several processing stages taking place in the depth of the cortex. The first stage, in layer 4C, is where the functional properties first emerge through a combination of thalamic afferent inputs and local intracortical circuitry. Once generated in this layer, a given functional property is then transferred to other layers in a columnar fashion, via interlaminar relays, where additional processing occurs.

We have also discussed the existence of a 'visible' anatomically defined column that is ~250–300 μm in diameter. This anatomical column is defined most clearly on the basis of reciprocal tangential connections within V1, and in terms of reciprocal inter-areal connections, rather than by having unique columnar circuits within its length. So what is the role of this anatomical column? The column appears to serve as a functionally tuned unit and point of information collation from laterally offset points. Information converges to the column from intracortical tangential connection fields in each layer, and from extra-striate feedback connections. Interactions between the column excitatory and inhibitory neurons, driven by thalamic inputs and inputs from other cortical columns within V1 and extra-striate areas, determine its neurons' receptive field properties and their modulation by surround stimuli.

Finally, we would like to suggest that the match in spatial scale of various anatomical substrates is an indicator of a common developmental origin. Commensurate with the basic width of a 2DG functional column are: (i) the diameter of the dendritic field of average-sized excitatory pyramidal neurons, (ii) the dendritic arbor size and axon arbor width of most of the inhibitory interneuron classes, (iii) the terminal zones of koniocellular thalamic axons in the CO blobs of layers 2/3, (iv) the width of columns or bands of terminals and cells of patchy tangential connections in all layers, and (v) the diameter of patches of cells making feedforward efferent projections to other cortical areas, and clusters of terminals made by feedback axons entering V1 from the same extra-striate cortical regions. To what extent these various connectivity patterns are generated by activity-based Hebbian mechanisms, such as those proposed for layer 4 of cat V1 (Kayser and Miller, 2002), is a subject for future research.

Notes

Our contributions to the findings described in this review have been supported over many years by grants from NEI, MRC, the Wellcome Trust, and most recently by Research to Prevent Blindness, Inc. to the Department of Ophthalmology, University of Utah. PCB would like to thank Jack D. Cowan for many helpful discussions. JSL and AA would like to thank Kesi Sainsbury for her excellent technical assistance in recent studies reported here.

Address correspondence to Jennifer S. Lund, Moran Eye Center, University of Utah, 50 North Medical Drive, Salt Lake City, UT 84132, USA. Email Jennifer.Lund@hsc.utah.edu.

References

Adorjan P, Levitt JB, Lund JS, Obermayer K (1999) A model of the intracortical origin of orientation preference and tuning in macaque striate cortex. Vis Neurosci 16:303–318.

Anderson JC, Martin KAC, Whitterridge D (1993) Form, function, and intracortical projections of neurons in the striate cortex of the monkey *Macacus nemestrinus*. Cereb Cortex 3:412–420.

Angelucci A, Levitt JB, Hupé J-M, Walton EJS, Bullier J, Lund JS (2000) Anatomical circuits for local and global integration of visual information: intrinsic and feedback connections. Eur J Neurosci 12 (Suppl. 11):285.

Angelucci A, Levitt JB, Lund JS (2002a) Anatomical origins of the classical receptive field and modulatory surround field of single neurons in macaque visual cortical area V1. Prog Brain Res 136:373–388.

Angelucci A, Levitt JB, Walton EJS, Hupé J-M, Bullier J, Lund JS (2002b) Circuits for local and global signal integration in visual cortex. J Neurosci 22:8633–8646.

Asi H, Levitt JB, Lund JS (1996) In macaque V1 lateral connections in layer 4B have a different topography than in layers 2/3. Soc Neurosci Abstr 22:1608.

Bauer U, Scholz M, Levitt JB, Lund JS, Obermayer K (1999) A model for the depth dependence of receptive field size and contrast sensitivity of cells in layer 4C of macaque striate cortex. Vis Res 39:613–629.

Ben-Yishai R, Lev Bar-Or, Sompolinsky H (1995) Theory of orientation tuning in visual cortex. Proc Natl Acad Sci USA 92:3844–3848.

Blasdel GG (1992a) Differential imaging of ocular dominance and orientation selectivity in monkey striate cortex. J Neurosci 12:3115–3138.

Blasdel GG (1992b) Orientation selectivity, preference, and continuity in monkey striate cortex. J Neurosci 12:3139–3161.

Blasdel GG, Fitzpatrick D (1984) Physiological organization of layer 4 in macaque striate cortex. J Neurosci 4:880–895.

Blasdel GG, Lund JS (1983) Termination of afferent axons in macaque striate cortex. J Neurosci 3:1389–1413.

Bonhoeffer T, Grinvald A (1991) Iso-orientation domains in cat visual cortex are arranged in pinwheel-like patterns. Nature 353:429–431.

Bressloff PC, Cowan JD (2002a) An amplitude equation approach to contextual effects in primary visual cortex. Neural Comput 14:493–525.

Bressloff PC, Cowan JD (2002b) A spherical model of orientation and spatial frequency tuning in a cortical hypercolumn. Philos Trans R Soc Lond B, in press.

Bressloff PC, Cowan JD, Golubitsky M, Thomas PJ, Wiener M (2001) Geometric visual hallucinations, Euclidean symmetry and the functional architecture of striate cortex. Philos Trans R Soc Lond B 356:299–330.

Buzas P, Eysel UT, Adorjan P, Kisvarday ZF (2001) Axonal topography of cortical basket cells in relation to orientation, direction and ocular dominance maps. J Comp Neurol 437:259–285.

Calford MB, Schmid LM, Rosa MGP (1999) Monocular focal retinal lesions induce short term topographic plasticity in adult cat visual cortex. Proc R Soc B 266:499–507.

Das A, Gilbert CD (1995) Receptive field expansion in adult visual cortex is linked to dynamic changes in strength of cortical connections. J Neurophysiol 74:779–792.

de Valois RL, de Valois KK (1988) Spatial vision. Oxford: Oxford University Press.

Dragoi V, Sur M (2000) Some properties of recurrent inhibition in primary visual cortex: contrast and orientation dependence on contextual effects. J Neurophysiol 83:1019–1030.

Ferster D, Chung S, Wheat H (1997) Orientation selectivity of thalamic input to simple cells of cat visual cortex. Nature 380:249–281.

Fitzpatrick D, Lund JS, Blasdel GG (1985) Intrinsic connections of macaque striate cortex: afferent and efferent connections of lamina 4C. J Neurosci 5:3350–3369.

Gilbert CD, Wiesel TN (1992) Receptive field dynamics in adult primary visual cortex. Nature 356:150–152.

Girard P, Hupé J-M, Bullier J (2001) Feedforward and feedback connections between areas V1 and V2 of the monkey have similar rapid conduction velocities. J Neurophysiol 85:1328–1331.

Girman SV, Sauve Y, Lund RD (1999) Receptive field properties of single neurons in rat primary visual cortex. J Neurophysiol 82:301–311.

Hawken MJ, Parker AJ (1984) Contrast sensitivity and orientation selectivity in laminar IV of the striate cortex of old world monkeys. Exp Brain Res 54:367–372.

Hawken MJ, Parker AJ, Lund JS (1988) Laminar organization and contrast sensitivity of direction-selective cells in the striate cortex of the Old-World monkey. J Neurosci 8:3541–3548.

Hubel DH, Wiesel TN (1962) Receptive fields, binocular interaction and functional architecture in the cat's visual cortex. J Physiol (Lond) 160:106–154.

Hubel DH, Wiesel TN (1974a) Sequence regularity and geometry of orientation columns in the monkey striate cortex. J Comp Neurol 158:267–294.

Hubel DH, Wiesel TN (1974b) Uniformity of monkey striate cortex: a parallel relationship between field size, scatter and magnification factor. J Comp Neurol 158:295–306.

Hubel DH, Wiesel TN (1977) Functional architecture of macaque monkey visual cortex. Proc R Soc Lond B 198:1–59.
Hubel DH, Wiesel TN, Stryker MP (1978) Anatomical demonstration of orientation columns in macaque monkey. J Comp Neurol 177:361–379.
Hübener M, Shoham D, Grinvald A, Bonhoeffer T (1997) Spatial relationships among three columnar systems in cat area 17. J Neurosci 17:9270–9284.
Humphrey AL, Hendrickson AE (1983) Background and stimulus-induced metabolic activity in the visual cortex (area 17) of the squirrel and macaque monkey. J Neurosci 3:345–358.
Hupé J-M, James AC, Payne BR, Lomber SG, Girard P, Bullier J (1998) Cortical feedback improves discrimination between figure and background by V1, V2 and V3 neurons. Nature 394:784–787.
Issa NP, Trepel C, Stryker MP (2000) Spatial frequency maps in cat visual cortex. J Neurosci 20:8504–8514.
Kapadia MK, Westheimer G, Gilbert CD (1999) Dynamics of spatial summation in primary visual cortex of alert monkeys. Proc Natl Acad Sci USA 96:12073–12078.
Kayser AS, Miller KD (2002) Opponent inhibition: a developmental model of layer 4 of the neocortical circuit. Neuron 33:131–142.
Levitt JB, Lund JS (2002) The spatial extent over which neurons in macaque striate cortex pool visual signals. Vis Neurosci, in press.
Livingstone MS, Hubel DH (1984a) Anatomy and physiology of a color system in the primate visual cortex. J Neurosci 4:309–356.
Livingstone MS, Hubel DH (1984b) Specificity of intrinsic connections in primate primary visual cortex. J Neurosci 4:2830–2835.
Lund JS (1987) Local circuit neurons of macaque monkey striate cortex. I. Neurons of laminae 4C and 5A. J Comp Neurol 257:60–92.
Lund JS, Wu CQ (1997) Local circuit neurons of macaque monkey striate cortex: IV. Neurons of laminae 1–3A. J Comp Neurol 384:109–126.
Lund JS, Yoshioka T (1991) Local circuit neurons of macaque monkey striate cortex. III. Neurons of laminae 4B, 4A and 3B. J Comp Neurol 311:234–258.
Lund JS, Lund RD, Bunt AH, Hendrickson AE, Fuchs A (1975) The origin of efferent pathways from the primary visual cortex, area 17, of the Macaque monkey as shown by retrograde transport of horseradish peroxidase. J Comp Neurol 164:287–303.
Lund JS, Fitzpatrick D, Humphrey AL (1985) The striate visual cortex of the tree shrew. In: Cerebral cortex (Peters A, Jones EG, eds), pp. 157–205. New York: Plenum.
Lund JS, Hawken, MJ, Parker AJ (1988) Local circuit neurons of macaque striate cortex. II Neurons of laminae 5B and 6. J Comp Neurol 276:1–29.
Lund JS, Yoshioka T, Levitt JB (1993) Comparison of intrinsic connectivity in different areas of macaque monkey cerebral cortex. Cereb Cortex 3:148–162.
Lund JS, Wu Q, Hadingham PT, Levitt JB (1995) Cells and circuits contributing to functional properties in area V1 of macaque monkey cerebral cortex: bases for neuroanatomically realistic models. J Anat (Lond) 187:563–581.
Lund JS, Angelucci A, Walton EJS, Bullier J, Hupé J-M, Girard P, Levitt JB (1999) Topographic logic of connections within and between macaque monkey visual cortical areas V1, V2, and V5. Invest Opthalmol Vis Sci S645:3397.
Malach R, Amir Y, Harel M, Grinvald A (1993) Relationship between intrinsic connections and functional architecture revealed by optical imaging and *in vivo* targeted biocytin injections in primate striate cortex. Proc Natl Acad Sci USA 90:10469–10473.
McGuire B, Gilbert C, Rivlin P, Wiesel TN (1991) Targets of horizontal connections in macaque primary visual cortex. J Comp Neurol 305:370–392.
McLaughlin DR, Shapley R, Shelley M, Wielaard J (2000) A neuronal network model of macaque primary visual cortex (V1): orientation selectivity and dynamics in the input layer 4Ca. Proc Natl Acad Sci USA 97:8087–8092.
Mountcastle VB (1957) Modality and topographic properties of single neurons of cat's somatic sensory cortex. J Neurophysiol 20:408–434.
Nelson S, Toth LJ, Sheat B, Sur M (1994) Orientation selectivity of cortical neurons during extra-cellular blockade of inhibition. Science 265:774–777.
Nelson SB (1991) Temporal interactions in cat visual system. III. Pharmacological studies of cortical suppression suggest a presynaptic mechanism. J Neurosci 11:369–380.
Newsome WT, Mikami A, Wurtz RH (1986) Motion selectivity in macaque visual cortex. III Psychophysics and physiology of apparent motion. J Neurophysiol 55:1340–1351.
Obermayer K, Blasdel GG (1993) Geometry of orientation and ocular dominance columns in monkey striate cortex. J Neurosci 13: 4114–4129.
Powell TPS, Mouncastle VB (1959) Some aspects of the functional organisation of the postcentral gyrus of the monkey: a correlation of findings obtained in a single unit analysis with cytoarchitecture. Bull Johns Hopk Hosp 105:133–162.
Reid RC, Alonso JM (1995) Specificity of monosynaptic connections from thalamus to visual cortex. Nature 378:281–284.
Ringach DL, Hawken MJ, Shapley R (1997) Dynamics of orientation tuning in macaque primary visual cortex. Nature 387:281–284.
Rockland KS, Lund JS (1983) Intrinsic laminar lattice connections in primate visual cortex. J Comp Neurol 216:303–318.
Roerig B, Chen B (2002) Relationships of local inhibitory and excitatory circuits to orientation preference maps in ferret visual cortex. Cereb Cortex 12:187–198.
Sceniak MP, Ringach DL, Hawken MJ, Shapley R (1999) Contrast's effect on spatial summation by macaque V1 neurons. Nat Neurosci 2:733–739.
Schmuel A, Korman M, Harel M, Grinvald A, Malach R (1998) Relationship of feedback connections from area V2 to orientation domains in area V1 of the primate. Soc Neurosci Abstr 24:767.
Shipp S, Zeki S (1989) The organization of connections between areas V5 and V1 in macaque monkey visual cortex. Eur J Neurosci 1:309–332.
Sillito AM, Kemp JA, Milson JA, Berardi N (1980) A re-evaluation of the mechanisms underlying simple cell orientation selectivity. Brain Res 194:517–520.
Sincich LC, Horton JC (2002) Divided by cytochrome oxidase: a map of the projections from V1 to V2 in macaques. Science 295:1734–1737.
Sokoloff L, Reivich M, Kennedy C, Des Rosiers MH, Patlak CS, Pettigrew KD, Sakurada O, Shinohara M (1977) The [14C] deoxyglucose method for the measurement of local cerebral glucose utilization: theory, procedure, and normal values in the conscious and anesthetized albino rat. J Neurochem 28:897–916.
Somers DC, Nelson S, Sur M (1995) An emergent model of orientation selectivity in cat visual cortical simple cells. J Neurosci 15:5448–5465.
Somers DC, Todorov EV, Siapas AG, Toth LJ, Kim D-S, Sur M (1998) A local circuit approach to understanding integration of long-range inputs in primary visual cortex. Cereb Cortex 8:204–217.
Somogyi P, Kisvarday ZF, Martin KAC, Whitteridge D (1983) Synaptic connections of morphological identified and physiologically characterised large basket neurons in the visual cortex of cat. Neurosci 10:261–194.
Somogyi P, Tamas G, Lujan R, Buhl EH (1998) Salient features of synaptic organisation in the cerebral cortex. Brain Res Rev 26:113–135.
Stetter M, Bartsch H, Obermayer K (2000) A mean field model for orientation tuning, contrast saturation and contextual effects in the primary visual cortex. Biol Cybern 87:291–304.
Tootell RBH, Hamilton SL, Switkes E (1988) Functional anatomy of macaque striate cortex. IV. Contrast and magno-parvo streams. J Neurosci 8:1594–1609.
Tsodyks M, Kenet T, Grinvald A, Arieli A (1999) Linking spontaneous activity of single cortical neurons and the underlying functional architecture. Science 286:1943–1946.
Yabuta NH, Callaway EM (1998) Cytochrome oxidase blobs and intrinsic horizontal connections of layer 2/3 pyramidal neurons in primate V1. Vis Neurosci 15:1007–1027.
Yoshioka T, Blasdel GG, Levitt JB, Lund JS (1992) Patterns of lateral connections in macaque visual area V1 revealed by biocytin histochemistry and functional imaging. Soc Neurosci Abstr 18:299.
Yoshioka T, Levitt JB, Lund JS (1994) Independence and merger of thalamocortical channels within macaque monkey primary visual cortex: anatomy of inter-laminar connections. Vis Neurosci 11:467–489.
Yoshioka T, Blasdel GG, Levitt JB, Lund JS (1996) Relation between patterns of intrinsic lateral connectivity, ocular dominance and cytochrome oxidase reactive regions in macaque monkey striate cortex. Cereb Cortex 6:297–310.
Yousef T, Toth E, Rausch M, Eysel UT, Kisvarday ZF (2001) Topography of orientation center connections in the primary visual cortex of the cat. Neuroreport 12:1693–1699.